Lab on a Chip

Accepted Manuscript

ROYAL SOCIETY OF CHEMISTRY

www.rsc.org/loc

Graphical abstract:

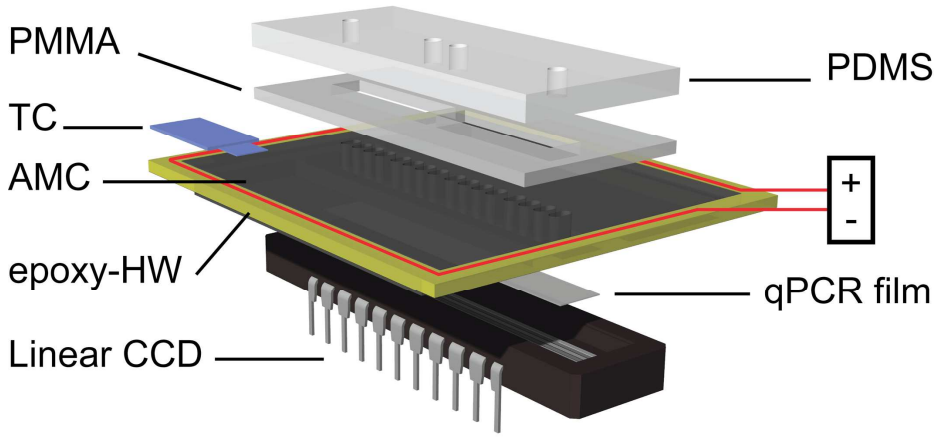

This is a portable system for water contamination monitoring. Using whole-cell as the biosensors, we integrate temperature control, microfluidic sample introduction, bioluminescence detection, and recording software into a complete system.

Water pollutant monitoring by whole cell array through lens-free detection on CCD

Hsieh-Fu Tsai[a], Yi-Ching Tsai[a], Sharon Yagur-Kroll[b], Noa Palevsky[b], Shimshon Belkin[b] and Ji-Yen Cheng[a,c,d,e,f*]

[a] Research Center for Applied Sciences, Academia Sinica, Taipei 11529, Taiwan
[b] Department of Plant and Environmental Sciences, The Alexander Silberman Institute of Life Sciences, The Hebrew University of Jerusalem, Jerusalem 91904, Israel
[c] Institute of Biophotonics, National Yang-Ming University, Taipei 11221, Taiwan
[d] Biophotonics & Molecular Imaging Research Center (BMIRC), National Yang-Ming University, Taipei 11221, Taiwan
[e] Department of Mechanical and Mechatronic Engineering, National Taiwan Ocean University, Keelung 20224, Taiwan
[f] Ph.D. Program in Microbial Genomics, National Chung Hsing University, 402, Taichung, Taiwan

* Corresponding author: Ji-Yen Cheng, Tel:+886 2 27873136; E-mail address: jycheng@gate.sinica.edu.tw

Abstract

Environmental contamination has become a serious problem to human and environmental health, as the exposure to a wide range of possible contaminants is continuously on the increase due to industrial and agricultural activities. Whole cell sensors have been proposed as a powerful tool to detect class-specific toxicants based upon their biological activity and bioavailability. We demonstrated a robust toxicant detection platform based on a bioluminescence whole cell sensor array biochip (LumiChip). LumiChip harbors an integrated temperature control and a 16-member sensor array, as well as a simple but highly efficient luminescence collection setup. On LumiChip, samples were infused in an oxygen-permeable microfluidic flow channel to reach the sensor array. Time-lapse changes in the bioluminescence emitted by the array members were measured on a single window-removed linear charge-coupled device (CCD) commonly used in commercial industrial process control or in barcode readers. Removal of the protective window on the linear CCD allowed lens-free direct interfacing of LumiChip to the CCD surface for measurement with high light collection efficiency. Bioluminescence induced by simulated contamination events was detected within 15 to 45 minutes. The portable LumiSense system utilizing the linear CCD in combination with the miniaturized LumiChip is a promising potential platform for on-site environmental monitoring of toxicant contamination.

Keywords

Bioluminescence, Whole Cell Biosensor, Environmental Toxicant Monitoring, Lens-free Detection, Linear CCD, Microfluidic Chip

1 Introduction

Increasing water pollution by contaminants from human activities poses threats to the ecosystem as well as to human health. Conventional methods for water quality analysis involve diverse chemical and physical methods. Although these methodologies offer sensitive and highly accurate determination of water quality, they require costly and sophisticated instrumentation in a well-controlled laboratory environment, as well as highly skilled personnel [1].

Whole cell sensors based on genetically engineered microorganisms have been proposed as a powerful tool for pollutant bioavailability determination [2–4]. Whole cell sensors have the advantages of miniaturization, portability, and rapid responses to class-specific chemicals [5–7]. Such bacterial bioreporters are molecularly engineered by fusing a gene promoter DNA element, known to be activated by the target compound(s), to reporter genes the products of which can be quantitatively monitored either by their activity or their quantity. The transduction mechanisms most often used as reporter activities in whole cell sensors are either electrochemical or optical [8]. In optical transduction, bacterial bioluminescence genes (*luxCDABE*) and fluorescent protein genes (for example green fluorescent protein) are popular choices, particularly because bacterial luciferases (when the *luxCDABE* gene cassette is used) and fluorescent proteins do not require the addition of external substrates. The bacterial luciferase encoded by the *luxAB* genes is a monooxygenase that oxidizes flavin mononucleotide and long chain aldehydes using molecular oxygen, generating blue-green bioluminescence at a wavelength of about 490 nm [9,10].

A variety of optoelectronic detection systems have been used for quantifying bioluminescence from whole cell sensors. The conventional method uses a luminometer equipped with photomultiplier tubes (PMTs) [11–13]. Bioluminescence can also be transferred through fiber-optic cables to the PMTs [14,15]. Another option is the use of highly sensitive avalanche photodiodes (APDs) [16,17]. The detection platforms based on PMTs and APDs share several disadvantages, including relatively bulky optics and the need for serial sample measurement by motorized scanning.

Solid state optoelectronic sensors with high field of view (FOV) such as charge-coupled device (CCD) and complementary metal oxide semiconductor (CMOS) cameras[18–20] have been used to simultaneously measure the bioluminescence from multiple whole cell sensors or lens-free (proximity-focused[21]) fluorescence microscopy. For lab-on-a-chip applications, lens-free configuration is of particular interest for its simplicity and

miniaturization. In lens-free fluorescence microscopy on CCD camera with high FOV, high-resolution fluorescent images can be obtained following compressive decoding of the raw image[22–27]. Bioluminescence measurement by the more expensive Peltier (thermoelectric)-cooled CCDs in either a wide-field optical configuration [28] or a lens-free configuration with the aid of fiber-optic taper have also been reported[29–31]. The former setup suffers from low numerical aperture due to the distance between the sample and the camera. The latter requires an expensive fiber-optic taper on which both ends are covered with cover glasses that could cause loss in spatial resolution.

In this study, we propose a miniaturization strategy of a bioluminescent whole cell sensor array biochip with integrated temperature-control components (LumiChip). The portable measurement system (LumiSense) allows direct lens-free interfacing of LumiChip to a linear uncooled CCD with no optical component, and thus bioluminescence is measured with high light collection efficiency. The simultaneous measurement of the bioluminescent response to model toxicants of a 16-member whole cell sensor array was demonstrated.

2 Materials and Methods

2.1 LumiChip design

The LumiChip has three components: an oxygen-permeable poly dimethyl siloxane/poly-methyl methacrylate (PDMS/PMMA) lid (referred to as “permeable lid” below), an aluminum multi-well chip (AMC), and an optically clear sealing film (FIG. 1A)

The permeable lid was fabricated as follows. Two or four microfluidic channels were patterned using AutoCAD software and were cut on a 1 mm-thick PMMA sheet backed with a piece of double-sided tape (70 μm, 3M, USA) using a CO_2 laser scriber (V2000, LTT Corp, Taiwan). The detailed fabrication procedure has been published previously [32–36]. The PMMA surface was activated by oxygen plasma and then silanized with 5% 3-aminopropyl triethoxysilane (3-APTES, Sigma-Aldrich, USA) aqueous solution. A 2 mm-thick sheet of PDMS was cured at 80° C (A:B=10:1, Sylgard 184, Dow Corning, USA). The silanized PMMA sheet and PDMS sheet were bonded together after oxygen plasma activation [37]. Holes for sample introduction were punched using a biopsy punch (Miltex, Inc., USA), finishing the fabrication of the permeable lid.

The AMC was fabricated as follows. A 2.5 mm-thick aluminum block was fabricated by a computer numerical control (CNC) process to create the wells for bacteria-agar mixtures and the grooves to fit on the ceramic

package of the CCD. A layer of polyimide tape was covered around the peripheral edges of the aluminum block to isolate electrical conduction. Then a resistance heating wire (0.18 mm in diameter, FCHW2, Silver Kohki Co., ltd, Japan) was wrapped around the aluminum block and adhered by epoxy resin. An electric current passing through the wire heats the AMC and the temperature distribution in the AMC was observed to be homogeneous due to the excellent thermal conductivity of aluminum (about 200 W/m·K)(SUPPL. FIG. 1).

An optically clear sealing film (qPCR film, L x W x H = 31 x 4 x 0.1 mm, BL6167, BasicLife Biosciences, Taiwan) was employed to seal the bottom of the AMC. Careful choice of the optically clear sealing film is important, as the film must be highly transparent at the spectral range of the bacterial bioluminescence emission, approximately 490 nm.

2.2 LumiSense system setup

The LumiSense system consists of two subsystems, the temperature-control subsystem and the linear CCD. (Fig. 1B)

The temperature-control subsystem is composed of three components: a proportional-integral-derivative (PID) controller (TTM-J4, Toho Electronics, Japan), a K-type thermocouple (Tecpel Co., Ltd, Taiwan) attached to LumiChip, and a 3 Volt transformer for resistive heating (Kaming, Taiwan). The thermocouple is affixed to the surface of an aluminum multi-well chip (AMC, please see below) to measure its temperature. The PID controller regulates the AMC temperature through resistive heating at a precision of ±0.1°C. The AMC can be rapidly heated from room temperature to 37°C within 3 minutes.

A board level line-scan CCD camera (TCN-1304-U, Mightex Systems, USA) with a window-removed Toshiba TCD1304DG linear CCD sensor (Eureca Messtechnik GmbH, Germany) was used as the bioluminescence sensing element. The Toshiba TCD1304DG linear sensor has a high sensitivity of 160 V/lux·s with a sensing area of 3,648 pixels over 29.1 mm The pixel size is 8 μm x 200 μm. The CCD socket was separated from its control board and put in a black plastic box to block ambient light. The window-removed linear CCD allowed the direct interface of LumiChip to the CCD surface for maximum spatial resolution. To prevent potential mechanical damage to the CCD, a conformal coating of Plastik 70 acrylic resin (CRC Industries, USA) was applied to the surface and the bonded wires were protected by epoxy resin.

2.3 Maintenance and preservation of bacterial strains

Escherichia coli bioreporter strains harboring plasmids containing fusions of stress-responsive gene promoters to *Photorhabdus luminescens luxCDABE* bioluminescence genes were used in this study (TABLE 1). The *E. coli* strains were streaked out on lysogeny broth (LB) agar plates (BD, USA) supplemented with 100 μg/mL ampicillin (Sigma-Aldrich, USA). Following overnight growth, the plates were kept at 4°C for toxicant stimulation experiment.

To preserve bacterial strains, a single colony was cultured overnight at 37°C in LB broth with 100 μg/mL ampicillin, mixed with glycerol to a final concentration of 25 % (W/V), and stored at -80°C.

2.4 Preparation of whole cell sensors on LumiChip

Two types of reporter cells were used in this study (TABLE 1), one harboring a *recA::luxCDABE* and the other a *yqjF::luxCDABE* fusion, tailored to respond to the presence of either genotoxic or nitroaromatic compounds, respectively [38,39]. For the sensing experiment, a single colony was picked from the LB agar plate, inoculated in LB broth supplemented with 100 μg/mL ampicillin, and grown overnight at 37°C. Bacterial suspension aliquots (20 μL) were further inoculated into fresh LB broth without ampicillin (1:100 dilution). The new suspension was then grown at 37°C with shaking (120 rpm) until optical density at 600 nm (OD_{600}) reached 0.2. The bacterial suspension was then concentrated to 10 fold by centrifugation at 16,100xg for 2 min and resuspension of the bacterial pellet in fresh LB medium. The bacterial suspension was then mixed with 2% molten LB agar on a 42°C dry bath to a working suspension with a final agar concentration of 0.5%.

After affixing the qPCR film to the bottom of the AMC, the bacterial suspensions were pipetted into the wells of the AMC, avoiding the formation of bubbles to prevent misidentification of well position and incorrect loading volume. The permeable lid was then affixed on the AMC through the double sided tape to complete the assembly of LumiChip.

The LumiChip was then mounted on the CCD sensor and the thermocouple was affixed to its surface. The LumiChip was then encompassed by a custom-made aluminum frame to avoid slipping, following which the electrical wires and the heating wire were connected.

2.5 Model toxicant stimulation

Prior to the measurement of the bioluminescence signal, the exact position of the wells were registered to the CCD sensor. For this purpose, a

light source (photoluminescent tape, Sign Kraft, USA) was adhered to the inner side of the black box's cover. The cover was then put in position so that the photoluminescent tape was placed above LumiChip. The light passing through LumiChip was detected by the CCD sensor and the well position profile was then acquired by the program LumiLogger (please see below).

After the position registration, the photoluminescent tape was removed. The time-lapse bioluminescence of the reporter cells was then acquired using LumiLogger with the maximum exposure time set at 6.5s. 0Model toxicants used for the simulation were nalidixic acid (NA, Sigma-Aldrich, USA) or hydroquinone (Q, Sigma-Aldrich, USA) dissolved in LB broth. The sample solutions were pipetted into the microfluidic channels in the permeable lid. The samples were loaded during an interval of the time-lapse data acquisition to avoid interference to the acquisition. Adhesive tape was then used to cover the sample holes to prevent evaporation. The experiments were performed in triplicate. Also, in each experiment, controls and non-specific strains were included to verify no cross-reaction and non-specific bioluminescence.

To study the effect of bacterial concentration on bioluminescence response kinetics, the bacteria suspensions at different cell densities were prepared as previously described. Cell concentration was determined by colony forming unit (CFU) counts of serially diluted samples spread on LB agar plates.

To study the effect of incubation temperature, the bacteria-agar mixtures of the *recA::lux* and *yqjFB2A1::lux* reporter strains were loaded onto four AMCs. The bioluminescent response to NA and hydroquinone was tested sequentially on the same LumiSense system at 22°C, 27°C, 32°C, and 37°C. The AMCs in queue were incubated in a humid environment at 4°C until used for bioluminescence.

2.6 LumiLogger software for bioluminescence data acquisition

A Python program (LumiLogger) with graphical user interface utilizing PyQT, NumPy, Matplotlib, and SciPy libraries was developed for this study (SUPPL. FIG. 2). To register the position of each well, LumiLogger first identified the start pixel and the end pixel defined as the pixel position that displayed 1/10 of the peak intensity of each well. LumiLogger acquires data from the linear CCD using exposure time set by the user. During time-lapse acquisition, LumiLogger automatically acquires triplicate data values at each time point and plots the intensity integral (*i.e.* area under the curve) of

each well as line plots. The integral was quantified by Simpson's rule.

2.7 Data analysis and statistics

The raw data were organized by using software packages Prism (GraphPad, USA) and OriginPro (OriginLab, USA). In all figures, data means were plotted with error bars representing 95% confidence interval.

Two-way analysis of variance (ANOVA) with repeated measures was used in the analysis. Time and either bacterial concentration, temperature, or toxicant concentration were within subject factors. When indicated by a statistically significant ANOVA test, differences were further investigated using a post-hoc Tukey's test. The significance level was set at $\alpha = 0.05$. P values smaller than 0.05, 0.01, 0.001, and 0.0001 are indicated by one, two, three, and four asterisks, respectively.

3 Results and discussion

3.1 Optimal spatial resolution by lens-free coupling of LumiChip to a linear CCD

In an AMC with 10 oval wells (L x W x H = 2 mm x 1.5 mm x 2.5 mm), the theoretical pixel span (dimensional pixel width, calculated by 1.5 mm X 3648 pixel / 29.1 mm = 188 pixels) for a well directly coupled to the CCD surface was 188 pixels. The actual pixel width (pixels with intensity larger than 3 times of baseline noise) of a peak acquired in an AMC with pristine surface (denoted as pristine AMC below) was 299 pixels, and the width identified by LumiLogger was 252 pixels. The identification by LumiLogger had included 84.3% of the actual pixel width into signal integration. However, the peak shape resembles a triangle, possibly due to the reflection of the luminescent light between the interior walls in the wells of the pristine AMC and the CCD sensor surface (FIG. 2A). To reduce internal light reflection, the pristine AMC was anodized to acquire a blackish appearance. For a black anodized AMC, the peak edges identified by LumiLogger were sharper than those in a pristine AMC. Moreover, a peak in the black anodized AMC had an actual pixel width of 225 pixels and the width identified by LumiLogger was 219 pixels. The identification encompassed 97.3% of the actual width (FIG. 2B). In the black anodized AMC, the actual pixel range (equivalent of 0.15 mm) of each peak was 20% larger than that of theoretical pixel range (225 / 188). This "blurring" suggested that the minimal spacing required to separate the signal from adjacent wells must be no less than 0.3 mm (= (225-188) x 29.1 / 3648). Theoretically, with a well width of 0.5 mm, a maximum of 36 (~= 29.1 / 0.8) reporter cells-containing wells can be integrated on a single AMC.

The minimum well-well distance on the AMC was also investigated by testing different well spacing from 0.5 mm to 1.0 mm. In a black anodized AMC, the sharp peak edge allowed evident well identification by LumiLogger even with a spacing of 0.5 mm (FIG. 2C). Separated signal peaks of each well were also apparent when the *yqjFB2A1::lux* strain was stimulated by hydroquinone (FIG. 2D). Appropriate well spacing is necessary both to allow adequate separation of signals from adjacent wells, as well as to allow firm adherence of the qPCR film to the AMC. In this study, we used AMCs designed with sixteen 4.5 µL oval wells (L x W x H= 2 x 1 x 2.5 mm) for an array of 16 members that can be simultaneously measured on a single linear CCD. The spacing between adjacent wells was 0.7 mm, to ensure firm adhesion of the qPCR film.

It has been shown that optoelectronic sensors can be used for lens-free imaging or detection of transmission light with a high spatial resolution and for realizing lab-on-chip applications[22,24–27,40–43]. On LumiSense system, we demonstrated that a simple windows-removed linear CCD can be used to detect the weak bioluminescence from the recombinant bacteria. In LumiChip, the bioluminescent bacteria cells in the wells can be considered as point light sources, and the average $\sin\theta$ in the well can be estimated. In 1 mm-wide wells of 16-member array LumiChip, the estimated upper limit of light collection efficiency is 28.5%. Shallower and wider wells would have higher light collection efficiency. However, shallower wells will contain less bacteria per well, and wider wells will limit the number of wells on a single chip. Detailed calculation of the collection efficiency is described in the supplementary information.

3.2 Power consumption of LumiSense system.

The line-scan CCD camera from Mightex is directly powered through the USB bus and does not require Peltier cooling component. The PID controller regulates the heating of the LumiChip. The miniaturization strategy that the LumiChip acts as both the reservoir and the incubation platform for whole cell sensor arrays is advantageous[29,44]. The miniaturization of the entire system is possible and the power consumption for heating can be decreased. Miniaturization and reduced power consumption are both important factors for portable instruments. We measured the electrical current consumed by LumiSense at 110V and calculated its power consumption. When the heater was operated at 100% duty cycle (initial phase of the experiment), the current was of 47.6±0.4 mA. After the temperature reached 37°C (within 3 minutes), the

LumiSense entered the regulated stage, under which the heater's duty cycle was approximately 50%. The current consumed when the heater was off was 16.6±0.3 mA. The average power consumption of LumiSense in regulation was thus 3.53 W (= 1/2 x (110 V x (47.6+16.6) mA)). In conclusion, the average power consumption of LumiSense system was expected to be lower than 4W over the 2-hour experiment, making it suitable for portable measurements.

3.3 Appropriate concentration of bacteria yields optimum bioluminescent response to toxicant

In this study, the bacterial strains were cultured to OD_{600} = 0.2 for optimal biological activity and then concentrated by centrifugation. The bioluminescent responses of different concentrations of reporter strains *recA::lux* and *yqjFB2A1::lux* in AMC induced by the model stimulants are shown in FIG. 3A and FIG. 3B.

For *recA::lux*, the data show that higher cell densities resulted in shorter response time, but that at concentrations higher than about $5x10^8$ CFU/mL, the maximal luminescence intensity decreased, probably due to lack of oxygen. A similar phenomenon was also observed for *yqjFB2A1::lux*. These results indicate that higher bacterial concentrations do not necessarily confer an advantage, and that cell density optimization is required for maximal luminescence intensities and shorter response times.

In the current study, the number of the bacteria in each well is about $2.25x10^6$ CFU in a 4.5 μL well ($5x10^8$ CFU/mL), which is significantly smaller than those reported previously. For comparison, in the work by Polyak *et al.*, 1.5~3.0x10^7 cells have been used for optimal fiber-optic detection [15], Elad *et al.* have employed $1.5x10^8$ cells in 60 μL [17], and Roda *et al.*, have used approximately $4.5x10^8$ in 30μL (half of OD 0.6 bacterial suspension) [30]. The improvement in our study is attributed to the high collection efficiency of the lens-free optical configuration.

3.4 Temperature-dependent bioluminescent response to toxicants

The homogeneous LumiChip temperature, provided by its integrated temperature control components, is crucial for maintaining the ability of genetically engineered bacterial reporters to respond to the environmental toxicants. The effects of temperature on the induced bioluminescence of *recA::lux* and *yqjFB2A1::lux* are shown in FIG. 4A and FIG. 4B.

For *recA::lux*, there is no bioluminescence at 22°C after 120 min of NA induction. At higher temperatures, the background signal increased,

probably due to the increase of thermal noise of the CCD sensor. However, at the higher temperatures induced bioluminescence intensity also increased and the response time was shortened. By ANOVA analysis, the time for a statistically significant bioluminescence response (p<0.0001) was 99 min, 51 min, 48 min for *recA::lux* stimulated at 27°C, 32°C, and 37°C, respectively.

For *yqjFB2A1::lux*, the induced bioluminescent by hydroquinone is stronger and the time to response is shorter compared to *recA::lux* induced by NA. These differences stem from the different mode of action of the *recA* and *yqjF* gene promoters [39,45]. The time for a statistically significant bioluminescence response (p<0.0001) was 45 min, 24 min, 24 min, and 15 min stimulated at 22°C, 27°C, 32°C, and 37°C, respectively.

These results emphasize the importance of a precise temperature control for biological activity, and demonstrate the advantage over the devices lacking thermal regulation[30]. As *E. coli's* optimum culturing temperature is 37°C, this incubation temperature contributes to its activity so that the responses are stronger and faster. Heat lability may be a problem when luciferase genes from marine bacterial species were used as reporting genes [46]. However, the luciferase of *Photorhabdus luminescens*, the optimal temperature of which is also 37°C [45,47], is highly suitable for the LumiChip-based sensing.

3.5 The dynamic bioluminescence response to model toxicants

Permeable lids with four isolated microfluidic channels were used to test the bioluminescence of *recA::lux* and *yqjFB2A1::lux* induced by four toxicant concentrations on a single LumiChip. The sample volume in each microfluidic channel was 20 µL.

Lens-free interfacing to CCD sensor in combination with integrated heater allows bioluminescence dynamic during the time lapse experiment be measured, quantified and analyzed in real time. The dosage-dependent bioluminescent response of *recA::lux* against 0.5 µg/mL to 1000 µg/mL NA, and that of *yqjFB2A1::lux* against 0.2 µg/mL to 1000 µg/mL hydroquinone, is shown in FIG.5A and FIG.5B, respectively. The linearity of the bioluminescence response of the two strains at the lower concentration range between 0 µg/mL to 100 µg/mL is shown in FIG.5C for both strains at 63 min. The real time data quantification allows possible identification of positive results at the earliest time point which is beneficial for rapid test applications.

The detection limit of NA by *recA::lux* was 5 µg/mL, and a statistically

significant bioluminescence change was identified at 63 min after the introduction of the toxicant (SUPPL. TABLE. 1). The detection limit of hydroquinone by *yqjFB2A1::lux* was 2 μg/mL and a statistically significant bioluminescence change was identified at 45 minutes after induction (p<0.01) (SUPPL. TABLE. 1). The induced bioluminescence at 120 min of both *recA::lux* and *yqjFB2A1::lux* to different concentrations of respective model toxicants is shown in supplementary information (SUPPL. FIG. 3A, 3B). Both strains had dose-dependent responses up to 100 μg/mL (SUPPL. FIG. 3C, 3D). The bioluminescence decreased at higher toxicant concentrations presumably due to toxic effect to the bacteria.

3.6 The repeatability and reproducibility of LumiChip

The measurement repeatability of the same test well was analyzed by coefficient of variation (CV) of the luminescence intensity. The CV was 8.54±0.37% for *recA::lux* and 4.18±0.13% for *yqjFB2A1::lux*. The variation was already considered during the two-way ANOVA statistical inference. The inter-test well repeatability evaluated by CV was 12.6± 0.67% for *recA::lux* and 11.53±0.58% for *yqjFB2A1::lux*. The inter-chip reproducibility in CV was also assessed to be 13.37±0.90% for *recA::lux* and 12.38±0.91% for *yqjFB2A1::lux.*

In this study, the bioluminescence was detected by a commercial linear CCD without Peltier cooling. Also, direct interfacing of the 37°C LumiChip to the sensor surface increased the thermal noise that contributes to the high CV. In the future, the repeatability and reproducibility can be improved through more precise control of bacterial number in the wells as well as an additional Peltier cooler for the linear CCD to suppress the thermal noise.

4 Conclusion

In this study, we demonstrated that the LumiChip and LumiSense provide a robust, portable, and miniaturized platform that could be used for on-site water contamination testing by an array of bacterial whole cell sensors. Using this system, the activities of a 16-member array of bioluminescent microbial sensors were simultaneously monitored on a chip with a single linear CCD in a lens-free imaging configuration. The lens-free configuration provided high light collection efficiency in a simple optical setup. The same lens-free interfacing of microfluidic chip with linear sensor could be beneficial for other lab-on-chip applications requiring both the

sensitivity and miniaturization. The reported LumiChip acted as both the reservoir for sensor array and the platform for temperature incubation. The integration realizes the miniaturization, optimal bacterial activity, sensitive bioluminescence detection, and low power consumption. Such integration is ideal for portable instruments. Although removal of the protective glass on the CCD increases the risk of damaging the sensor by electrostatic discharge, proper grounding and handling could prevent such damages, as demonstrated in this work. While in the present study we have only employed two bioreporter cell types, the 16-well configuration potentially allows the inclusion of up to 16 different sensor strains, thus providing a broad-spectrum coverage of different toxicant classes

In the future, LumiChip will be modified to include a continuous flow channel and integrated pumping components, enabling online monitoring of water pollution [12,17]. By integrating miniaturized electronics, handheld and low power consuming LumiSense system can be created. Also, by incorporating appropriate excitation light source and thin film filter, fluorescent whole cell sensors may also be used on the portable platform [48]. Models of toxicant induction pattern [49] or time-lapse statistical inference could be included in the dedicated Python program, LumiLogger, for determining positive tests automatically during the experiment.

5 Acknowledgement

The authors would like to thank Dr. Yi-Chung Tung of Research Center for Applied Sciences, Academia Sinica for his support on equipment and Mr. Ben Gamari at University of Massachusetts, USA for his work on Python interface for line CCD. The work is financially supported by a Taiwanese-Israeli grant for scientific research cooperation administered by the Israeli Ministry of Science and by the Taiwanese Ministry of Science and Technology (NSC 102-2923-M-001-004-MY2) and by the Research Program on Nanoscience and Nanotechnology, Academia Sinica, Taiwan, and by the Hebrew University-Academia Sinica Joint Research Program on Nanoscience and Nanotechnology.

6 References:

1 S. Belkin, *Curr. Opin. Microbiol.*, 2003, **6**, 206–212.

2 S. Köhler, S. Belkin and R. D. Schmid, *Fresenius J. Anal. Chem.*, 2000, **366**, 769–779.

3 J. R. van der Meer and S. Belkin, *Nat. Rev. Microbiol.*, 2010, **8**, 511–522.

4 M. Woutersen, S. Belkin, B. Brouwer, A. P. van Wezel and M. B. Heringa, *Anal. Bioanal. Chem.*, 2011, **400**, 915–929.
5 S. Daunert, G. Barrett, J. S. Feliciano, R. S. Shetty, S. Shrestha and W. Smith-Spencer, *Chem. Rev.*, 2000, **100**, 2705–2738.
6 S. Girotti, E. N. Ferri, M. G. Fumo and E. Maiolini, *Anal. Chim. Acta*, 2008, **608**, 2–29.
7 M. B. Gu, R. J. Mitchell and B. C. Kim, in *Biomanufacturing*, ed. J.-J. Zhong, Springer Berlin Heidelberg, 2004, pp. 269–305.
8 E. Eltzov and R. S. Marks, *Anal. Bioanal. Chem.*, 2011, **400**, 895–913.
9 S. Forst, B. Dowds, N. Boemare and E. Stackebrandt, *Annu. Rev. Microbiol.*, 1997, **51**, 47–72.
10 M. J. Cormier and J. R. Totter, *Biochim. Biophys. Acta*, 1957, **25**, 229–237.
11 S. Belkin, D. R. Smulski, A. C. Vollmer, T. K. V. Dyk and R. A. LaRossa, *Appl. Environ. Microbiol.*, 1996, **62**, 2252–2256.
12 M. Bock Gu and G. Cheol Gil, *Biosens. Bioelectron.*, 2001, **16**, 661–666.
13 R. Daniel, R. Almog, Y. Sverdlov, S. Yagurkroll, S. Belkin and Y. Shacham-Diamand, *Appl. Opt.*, 2009, **48**, 3216–3224.
14 J. H. Lee and M. B. Gu, *Biosens. Bioelectron.*, 2005, **20**, 1744–1749.
15 B. Polyak, E. Bassis, A. Novodvorets, S. Belkin and R. S. Marks, *Sens. Actuators B Chem.*, 2001, **74**, 18–26.
16 R. Daniel, R. Almog, A. Ron, S. Belkin and Y. S. Diamand, *Biosens. Bioelectron.*, 2008, **24**, 882–887.
17 T. Elad, R. Almog, S. Yagur-Kroll, K. Levkov, S. Melamed, Y. Shacham-Diamand and S. Belkin, *Environ. Sci. Technol.*, 2011, **45**, 8536–8544.
18 E. K. Bolton, G. S. Sayler, D. E. Nivens, J. M. Rochelle, S. Ripp and M. L. Simpson, *Sens. Actuators B Chem.*, 2002, **85**, 179–185.
19 S. K. Islam, R. Vijayaraghavan, M. Zhang, S. Ripp, S. D. Caylor, B. Weathers, S. Moser, S. Terry, B. J. Blalock and G. S. Sayler, *IEEE Trans. Circuits Syst. Regul. Pap.*, 2007, **54**, 89–98.
20 M. L. Simpson, G. S. Sayler, B. M. Applegate, S. Ripp, D. E. Nivens, M. J. Paulus and G. E. Jellison Jr, *Trends Biotechnol.*, 1998, **16**, 332–338.
21 E. Karplus, in *Photoproteins in Bioanalysis*, eds. S. Daunert and S. K. Deo, Wiley-VCH, Weinheim, 1 edition., 2006, pp. 199–223.
22 S. A. Arpali, C. Arpali, A. F. Coskun, H.-H. Chiang and A. Ozcan, *Lab. Chip*, 2012, **12**, 4968–4971.
23 A. F. Coskun, I. Sencan, T.-W. Su and A. Ozcan, *Opt. Express*, 2010, **18**, 10510–10523.
24 A. F. Coskun, I. Sencan, T.-W. Su and A. Ozcan, *PLoS ONE*, 2011, **6**, e15955.

25 A. F. Coskun, I. Sencan, T.-W. Su and A. Ozcan, *Analyst*, 2011, **136**, 3512–3518.
26 A. Ozcan and U. Demirci, *Lab. Chip*, 2007, **8**, 98–106.
27 A. F. Coskun, T.-W. Su and A. Ozcan, *Lab. Chip*, 2010, **10**, 824–827.
28 J.-M. Ahn and M. B. Gu, *Appl. Biochem. Biotechnol.*, 2012, **168**, 752–760.
29 A. Roda, L. Cevenini, S. Borg, E. Michelini, M. M. Calabretta and D. Schüler, *Lab. Chip*, 2013, **13**, 4881–4889.
30 A. Roda, L. Cevenini, E. Michelini and B. R. Branchini, *Biosens. Bioelectron.*, 2011, **26**, 3647–3653.
31 R. Ramji, C. F. Chiong, H. Hirata, A. R. A. Rahman and C. T. Lim, *Small*, 2014, DOI:10.1002/smll.201401674.
32 J.-Y. Cheng, C.-W. Wei, K.-H. Hsu and T.-H. Young, *Sens. Actuators B Chem.*, 2004, **99**, 186–196.
33 C.-W. Huang, J.-Y. Cheng, M.-H. Yen and T.-H. Young, *Biosens. Bioelectron.*, 2009, **24**, 3510–3516.
34 H.-F. Tsai, S.-W. Peng, C.-Y. Wu, H.-F. Chang and J.-Y. Cheng, *Biomicrofluidics*, 2012, **6**.
35 M. Z. Mousavi, H.-Y. Chen, S.-H. Wu, S.-W. Peng, K.-L. Lee, P.-K. Wei and J.-Y. Cheng, *Analyst*, 2013, **138**, 2740–2748.
36 J.-Y. Cheng, C.-J. Hsieh, Y.-C. Chuang and J.-R. Hsieh, *Analyst*, 2005, **130**, 931–940.
37 K. Kim, S. W. Park and S. S. Yang, *BioChip J.*, 2010, **4**, 148–154.
38 Y. Davidov, R. Rozen, D. R. Smulski, T. K. Van Dyk, A. C. Vollmer, D. A. Elsemore, R. A. LaRossa and S. Belkin, *Mutat. Res. Toxicol. Environ. Mutagen.*, 2000, **466**, 97–107.
39 S. Yagur-Kroll, C. Lalush, R. Rosen, N. Bachar, Y. Moskovitz and S. Belkin, *Appl. Microbiol. Biotechnol.*, 2014, **98**, 885–895.
40 A. Greenbaum, W. Luo, T.-W. Su, Z. Göröcs, L. Xue, S. O. Isikman, A. F. Coskun, O. Mudanyali and A. Ozcan, *Nat. Methods*, 2012, **9**, 889–895.
41 D. M. Vykoukal, G. P. Stone, P. R. C. Gascoyne, E. U. Alt and J. Vykoukal, *Angew. Chem.*, 2009, **121**, 7785–7790.
42 M. Li, D. N. Ku and C. R. Forest, *Lab. Chip*, 2012, **12**, 1355–1362.
43 Z. Göröcs and A. Ozcan, *Lab. Chip*, 2014, **14**, 3248–3257.
44 T. Charrier, C. Chapeau, L. Bendria, P. Picart, P. Daniel and G. Thouand, *Anal. Bioanal. Chem.*, 2011, **400**, 1061–1070.
45 S. Yagur-Kroll and S. Belkin, *Anal. Bioanal. Chem.*, 2011, **400**, 1071–1082.
46 K. Yagi, *Appl. Microbiol. Biotechnol.*, 2007, **73**, 1251–1258.
47 A. Westerlund-Karlsson, P. Saviranta and M. Karp, *Biochem. Biophys. Res. Commun.*, 2002, **296**, 1072–1076.

48 Y. Kabessa, V. Korouma, H. Ilan, S. Yagur-Kroll, S. Belkin and A. J. Agranat, *Biosens. Bioelectron.*, 2013, **49**, 394–398.

49 A. Rabner, E. Martinez, R. Pedhazur, T. Elad, S. Belkin and Y. Shacham, *Nonlinear Anal Model Control*, 2009, **14**, 505–529.

7 Figure Captions

FIG.1 (A) The LumiChip on top of the linear CCD. TC: Thermocouple. Epoxy-HW: heating wire embedded in epoxy resin. (B) The photopicture of LumiSense system.

FIG.2 (A) The well profile of a pristine AMC identified by LumiLogger (B) The well profile of a black anodized AMC identified by LumiLogger. (C) The well design with different spacing and the well profile identified by LumiLogger. (D) The bioluminescence of *yqjFB2A1::lux* stimulated by hydroquinone in the wells shown in (C).

FIG.3 (A) The temporal response of *recA::lux* luminescence at different bacteria concentration stimulated by NA. (B) The temporal response of *yqjFB2A1::lux* luminescence at different bacteria concentration stimulated by hydroquinone. In both panels, the Z axis indicates the bioluminescent signal integral (area under the curve).

FIG.4 (A) the bioluminescent response of *recA::lux* stimulated by 10 μg/mL NA at 22, 27, 32, 37 ˚C. (B) The bioluminescent response of *yqjFB2A1::lux* induced by 200 μg/mL hydroquinone at 22, 27, 32, 37 ˚C.

FIG.5 (A) The bioluminescence response of *recA::lux* to different concentrations of NA. (B) The bioluminescence response of *yqjFB2A1::lux* to different concentration of hydroquinone. (C) The linearity of bioluminescence response to different concentrations of stimulants of the two strains at 63 min.

8 Table

Bacterial reporter	Model inducer	Class of detected toxicants	Reference
recA::lux	Nalidixic acid (NA)	DNA damaging agents	[38]
yqjFB2A1::lux	Hydroquinone (Q)	di-nitrotoluene related compounds	[39]

TABLE.1 Two *E. coli* strains with plasmids containing reporter gene-*lux* fusions.

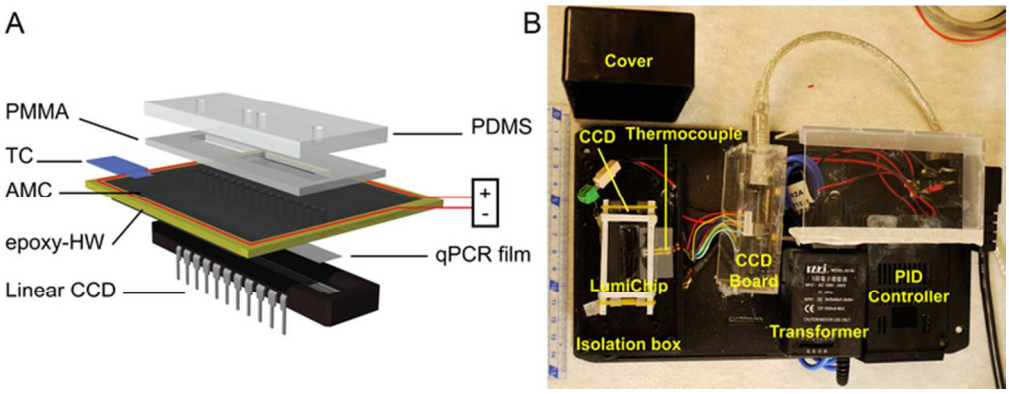

65x24mm (300 x 300 DPI)

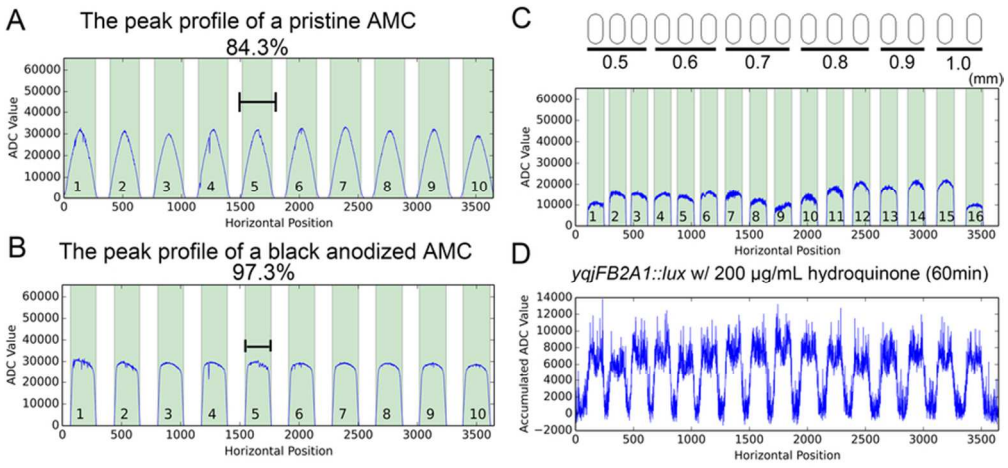

78x36mm (300 x 300 DPI)

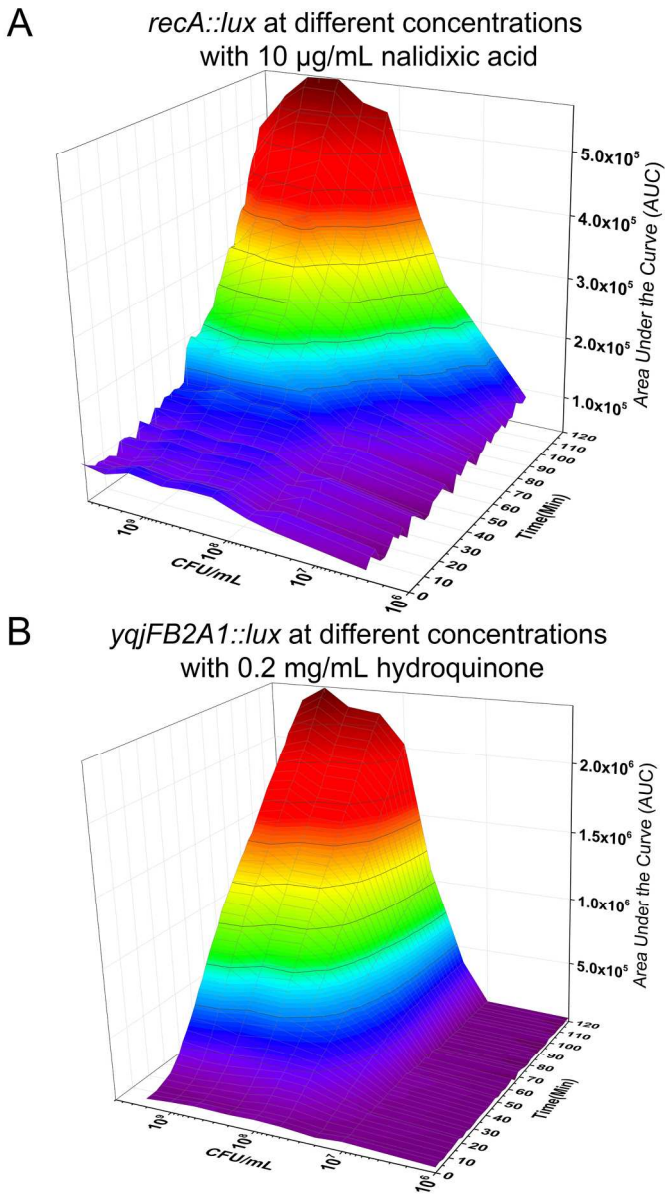

140x239mm (300 x 300 DPI)

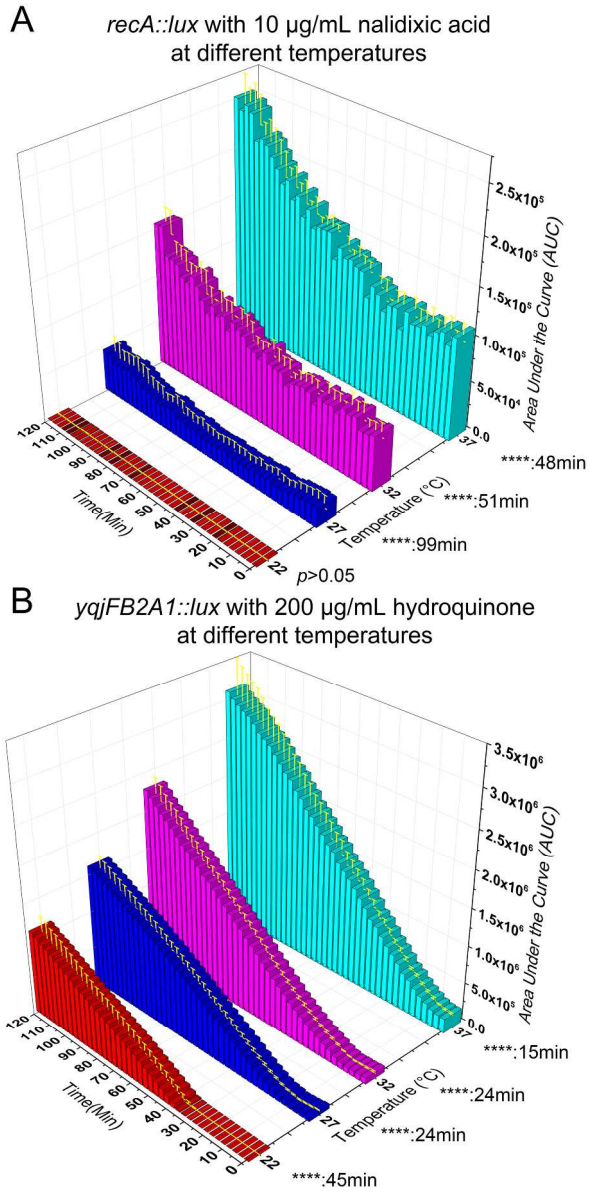

166x333mm (300 x 300 DPI)

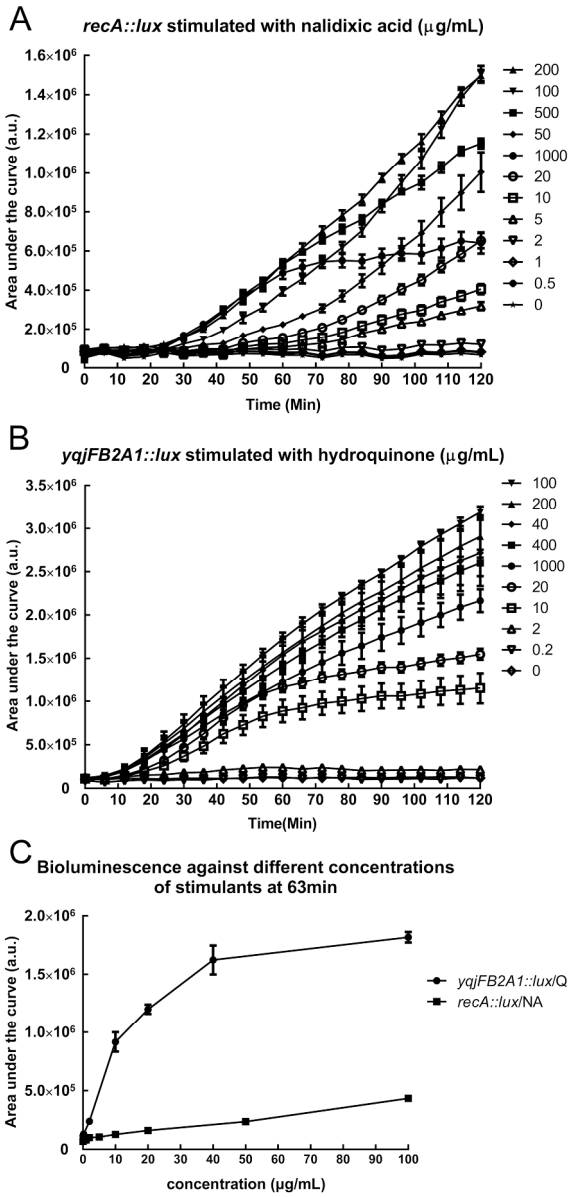

176x375mm (300 x 300 DPI)